ISSN: 2321-7782 (Online)
Volume 1, Issue 6, November 2013
International Journal of Advance Research in Computer Science and Management Studies
Research Paper
Available online at: www.ijarcsms.com

An Automated Image Segmentation Scheme for MRI

Dr. Saravana Kumar Ganesan[1]
Dept of Electronics & Communication Engg.
AMS college of Engineering
Erumapatti, Namakkal
Tamilnadu – India

Dr. L.C.S. Gowda[2]
Dept of Electronics & Communication Engg.
AMS college of Engineering
Erumapatti, Namakkal
Tamilnadu – India

Dr. Ravi Sundaram[3]
Dept of Electronics & Communication Engg.
AMS college of Engineering
Erumapatti, Namakkal
Tamilnadu – India

Dr. Fathima Jabeen[4]
Dept of Electronics & Communication Engg.
Islamia Institute of Technology
Bangalore
Karnataka – India

A. Natarajan[5]
Dept of ECE
AMS College of Engineering
Erumapatti, Namakkal
Tamilnadu – India

Abstract: ***This paper proposes a segmentation scheme for segmenting the brain from head magnetic resonance (MR) images. The scheme exhibits sturdiness to curb the influence of inhomogeneities caused by radio frequency (RF). The automation property ensures in segmenting the brain from each head image slice. The versatility of the scheme lies in managing images acquired from numerous different MRI scanners, using different-resolution images and different echo sequences. The method uses an integrated approach which utilizes adaptive non local filtering technique and contouring techniques, and a priori knowledge, which is used to remove offsets, which are delicate to obtain generalized image skeletonization. The scheme endorses two stage processes, comprising of eliminating background noise leaving a head mask, then pronouncing a coarse edge of the brain, then enhancement of the coarse brain outline to a final mask. The results obtained substantiate the aforementioned characteristics of the proposed algorithm.***

Keywords: Adaptive non local filtering, MRI brain, contouring.

I. INTRODUCTION

The comprehensive images of living tissues is endowed by Magnetic Resonance Imaging (MRI), and is utilized for both brain and body human studies. To identify tissue abnormalities such as cancers and injuries data obtained from MR images is used; MR is also used in widespread ways to study brain pathology, where feature localization are often examined in detail, for example in multiple sclerosis (MS) studies [36], [35]. The definition of the brain by feature localization is mandatory to perform good quantitative analysis. In conventional methods, a expert technician manually outlines the ROI's using a mouse or cursor. More recently, computer-assisted methods have been used for specific tasks such as extraction of MS lesions from MRI brain scans [23], [47], or extraction of the cerebral ventricles in schizophrenia studies [15]. Many of these computer-assisted tasks require segmentation of the whole brain from the head, either because the whole brain *is* the ROI such as in Alzhiemer's studies [18] or because automatic ROI extraction using statistical methods is made easier if the skull and scalp have been removed [23].

We describe our automatic method for segmenting the brain from the head in MR images. The key to any automatic method is that it must be robust; so that it produces reliable the key to any automatic method is that it must be robust, so that it produces reliable results on every image acquired from any MR scanner using different relaxation times, slice thicknesses and

fields of view. Our method is so robust, that it successfully was able to segment the brain in every slice of 40 head images from five different MRI scanners (all 1.5-T; four from GE, one from Siemens), using several different spin-echo images with different echo times, and with two T1-weighted gradient pulse sequences. Our method works in the presence of typical radio frequency (RF) in homogeneity and it addresses the partial volume effect in a consistent reasonable manner. The method is partly two-dimensional (2-D)-based and partly three-dimensional (3-D)-based, and it works best on routine axially displayed multispectral dual-echo proton density (PD) and T2 (spin-spin relaxation time) sequences. It also works well on axial and coronal 3-D T1-weighted SPGR (Spoiled Gradient) sequences. However, it does not work fully automatically on sagitally displayed 3-D T1-weighted images where accurate localization of cortical convolutions is required, as parameter tuning is necessary to include the thin dark brain areas and keep the cerebellum attached to the rest of the brain, while simultaneously separating the brain from the back of the neck tissue and the cheeks. For such sagitally displayed images, other techniques such as those described in [1], [13], [19], and [24] are available. The computer processing time for each study for all the stages was less than five minutes on a SUN SPARC workstation—even for the 120 slice 3-D studies. For segmentation of the brain, hybrid methods incorporating both image-processing and model-based techniques are useful [1], [4], [24]. Our hybrid method is typical in that it involves some image processing steps first: viz. a thresholding step followed by a morphological erosion to remove small connections between the brain and surrounding tissue. A model-based approach is then used to eliminate the eyes and other nonbrain features, followed by more image processing consisting of a morphological dilation to recover some of the eliminated tissue and a final refinement of the brain contour (in our case, using Terzopoulos and Kass's active contour algorithm [25]).

Our method is unique in that it is possible to select the image processing parameters automatically; in particular, the thresholding parameter is found by applying an anisotropic diffusion filter to the image and locating a threshold based on the characteristics of the resulting voxel intensity histogram.

II. Literature Survey

The survey by Clarke *et al.* of segmentation methods for MR images [11] describes many useful image processing techniques and discusses the important question of validation. The brain can be divided into several groups: those required to perform a crude threshold-based extraction of the brain, followed by refinement of brain contours; statistical methods for brain segmentation, and region growing methods.

A. Brain Extraction Using Automatic Thresholding

Suzuki and Toriwaki use iterative thresholding to distinguish brain tissues from others in axial MR slices [43]. Starting at set values, thresholds for the head and the brain are then iteratively adjusted based on the geometry of resulting masks (i.e., the head mask includes the brain mask). This method is ineffective in the presence of RF in homogeneity and in slices where the brain is not one homogeneous region closely surrounded by the skull. Li et al. use knowledge-based thresholding in multimodal MRI data to classify voxels into multiple intensity categories [27]. In each axial slice, they compute the centroid of voxels categorized as brain. Next, four points defining a quadrangle are found at the edge of the brain by tracing left, right, up, and down from the centroid to a transition in tissue categories. All voxels outside the quadrangle that are not categorized as brain tissue are then masked to define the intracranial contour. Obviously, this method works only in slices where the brain constitutes one fairly homogeneous region.

Brummer et al. use histogram analysis and morphology to generate a 3-D brain mask [8]. Using a model of background noise, they first automatically generate a mask of the head and perform intensity correction on the masked volume. Next they create an initial brain mask using an automatic threshold based on a presupposed brain voxel intensity distribution. They then eliminate regions in the brain mask that are too close to the edge of the head. Finally, they use novel morphological operations to clean up the resulting mask. This method misses brain tissue in extreme slices and includes nonbrain tissues in others. In

some cases it produces errors near the eyes. The method relies on a priori intensity correction to deal with RF in homogeneity, so cannot be used retroactively.

Aboutanos and Dawant [1] use histogram analysis to determine the threshold selection in 3-D T1-weighted magnetization-prepared rapid gradient echo (MP-RAGE) data sets where the grey matter appears darker than the white; they choose as a lower threshold the peak intensity of the grey matter, and an upper threshold in the vicinity of the upper boundary of the white matter, where the brain lobe starts to flatten. These parameters can be automatically located, but the resulting brain segmentation may underestimate the grey matter and may still allow attachment of the dura to the brain in certain images. Furthermore, their method for evaluating threshold values is unique to the MP-RAGE acquisition sequence. However, we have incorporated their thresholds for 3-D MP-RAGE volumes in our algorithm with some success, although our results have yet to be validated.

B. Refinement of Brain Contour

Aboutanos and Dawant [1] describe a geometric deformable model used to refine an initial brain mask. Their deformable model uses the pixel intensity along lines which are placed approximately perpendicular to the initial contour. A five-term cost matrix is associated with transforming the image to hug the contours; curve from image locations such as eye and skin locations in T1-weighted images. The authors have found values for these parameters which perform well on sagitally displayed brain contours of 3-D T1-weighted MP-RAGE volumes on many volunteers, although the method requires a very good initial contour and excess fat can affect results. Two iterations are applied, and the blurred image is used to reduce the effect of noise. This method looks very promising, but no results are presented for PD and T2-weighted images.

Chakraborty et al. combine statistical segmentation and boundary detection to isolate features in MR images [9]. They first segment the images using a method similar to the iterated conditional modes (ICM) algorithm [22]. They then use a parametrically deformable shape model algorithm to find the boundary of interesting features in the segmented image [41]. The shape model algorithm modifies the shape of a predefined closed contour to match the shape of a ROI. This method requires user interaction to seed the segmentation and provide an initial shape contour. Further, the segmentation may fail due to RF in homogeneity.

Snell et al. use an active surface template to find the intracranial boundary in MRI volumes of the head [40]. The method is based on the active contour model algorithm, "Snakes" [25]. Given an initial estimate of an object boundary, "Snakes" approaches the actual boundary by solving an energy minimization problem. In Snell's method, the user identifies points in the MR image that correspond to points on a "standard" active surface template of the brain. Based on these points, the template is registered to the image. The "Snakes" algorithm is then used to attract the surface template to the intracranial boundary. Snell's method appears to work better than all the other methods discussed herein. However, Snell used high-resolution isotropic 3-D MRI data to test his algorithm. Such MRI scans are generally not performed clinically. Still, the method requires user interaction and may fail for images that do not contain the entire brain.

Snakes have been used successfully to extract the contours from cardiac MRI studies [38] by propogating the snake from one image to another, with an intermediate processing step to provide a better starting contour, which prevents the snake contour from becoming trapped in incorrect local minima. This study highlights the need to provide a good initial contour for subsequent snake contour refinement; a lesson which we learnt early in our research too.

Davatzikos and Prince propose the use of a new active contour algorithm for ribbons (ACAR), which is specifically designed for mapping the human cortex [14]. Their initial results are promising, but the examples given are not visually superior to our results using snakes, although their method may prove better than snakes at tracking into cortical convolutions.

Lobregt and Viergever [30] propose a different dynamic contour model based on deformation of a set of vertices connected by edges. The deformation is caused by acceleration forces acting on the vertices; the forces are internal (derived from the shape of the contour model) and external (derived from some image feature energy distribution). At each deformation step, the new

position of each vertex is calculated; after a number of steps, a stable end situation is reached when both velocity and acceleration are zero for each vertex. Preliminary results applying this technique show its promise in tracking edges in 2-D medical images, although it is very sensitive to the initial contours provided.

Thedens et al. [44] proposed another method to search for borders in MR images, based on graph searching for minimum cost edge detection applied to a temporal or spatial sequence of images. This method has been shown to work on cardiac MR images, but it cannot be used on a single image volume—a sequence of several images is required—and it is computationally very expensive.

Lundervold and Storvik proposed a segmentation method for brain parenchyma in the central slices of multispectral MR images [31] which uses a model-based segmentation method and also uses a new Bayesian dynamic contour (BDC) model to detect the boundaries. The advantage of this approach over the snakes active contour is that the energy functions used to find the boundary can be more generally based on information about the whole region, rather than just the local boundary characteristics. The results are promising for the central slices of multispectral images presented, but have yet to be developed for isolating the whole brain or for working with just a single echo sequence.

Li et al. [28] have developed a knowledge-based segmentation technique called "segementation" which allows identification of the brain contours in computed tomography (CT) images, upon which they use a boundary refinement algorithm to improve the brain boundary. This algorithm maximizes an optimization function of the gradient, the orientation change of the gradient and the local curvature. The results are given for fairly smooth contours of the brain in axial CT slices, and it is not known if the algorithm is able to track the cortex in MR images.

Automatic skull boundary detection for the purposes of automatic registration of CT and MR head images has been developed by Van den Elsen et al. [16], based on the fact that the MRI signal forms a trough at the skull. In certain MRI slices the skull boundary is close to the brain boundary, but this cannot be used in general to segment the brain.

III. METHOD

The proposed method to segment the brain image from MRI is presented as follows.

A. Overview

We use a three-stage method to segment images as shown in Fig. 1. First we remove the background noise, then we generate an initial mask for the region(s) of interest, then we refine the mask for the final segmentation. Each stage (bubble) in the diagram has been implemented using the WiT visual programming environment [3], which aids prototype development and enables experimentation [5].

The first stage, Segment Head, uses intensity histogram analysis to remove background noise and provide a head mask defining the head. The second stage, Generate Initial Brain Mask, produces a mask that approximately identifies the intracranial boundary. A head image is filtered using a nonlinear anisotropic diffusion filter, to identify regions corresponding to the brain. The T2- weighted image is used if it is available; else the PD-weighted or T1-weighted image may be used. The nonlinear anisotropic diffusion effectively counters RF inhomogeneity by smoothing the brain regions and by reducing the intensity of the narrow nonbrain regions such as the scalp.

With the initial brain mask as a seed, the third step, Generate Final Brain Mask, locates the intracranial boundary using an active contour model algorithm. The active contour model algorithm consistently tracks the edge of the brain, even in the presence of partial volume effects.

Stages 1 and 3 require no a priori information about the organ to be segmented. Knowledge about the organ of interest is used only in the second stage, in which the initial brain mask is generated. We use two expert pieces of information. One allows us to eliminate no brain tissues such as the eyes, using morphology, by exploiting the simple fact that the brain centroid must be

near the centric of the slice. The other item of knowledge is that the brain tissues appear in MR images with relatively high intensity and when the T2 (or PD) image is filtered with a special anisotropic diffusion filter, most of the no brain tissues can be darkened, and hence the brain tissues can be segmented using a simple threshold. The methodology is described in more detail below and in full detail in [32]. Although seemingly complex, the method has proven so robust that it works even in the presence of RF in homogeneity, which would not be the case if a simple threshold technique were used to identify brain tissue from no brain tissue.

B. Segment Head

The head mask is generated using the method suggested by Brummer *et al.* to determine the "best" threshold level for removing background noise in PD-weighted MR images [8]. The method is based on the fact that MR scanners produce normally distributed white noise [17]. Henkelman [21] showed that background noise in reconstructed MR volumes has a Rayleigh distribution

$$p_{\text{noise}}(f) = \frac{f}{\sigma^2}\exp\left(-\frac{f^2}{2\sigma^2}\right)$$

Where f is the noise intensity and is the standard deviation of the white noise. Fig. 2 shows that this distribution is easily visible in the low intensity range of the uncorrected MRI histogram.

The subtraction of the best-fit Rayleigh curve, from the volume histogram produces a bimodal distribution

$$g(f) = h(f) - r(f)$$

A minimum error threshold can be determined from by minimizing an error term

$$\varepsilon_\tau = \sum_{f=0}^{\tau-1} g(f) + \sum_{f=\tau}^{\infty} r(f).$$

Fig. 3 shows the results of automatically thresholding an MR volume using this method. The binary image in Fig. 3(b) produced by thresholding the volume at, contains speckle outside the head region and has misclassified regions within the head. This "noise" is easily removed using standard morphological operations.

This is a three step process which first uses 2-D nonlinear anisotropic diffusion to smooth the brain and attenuate narrow non brain regions such as the scalp in each MRI slice. Next, it automatically thresholds the diffused MR volume to produce a binary mask. Finally, misclassified, non brain regions are removed from the binary mask using morphology and spatial information provided by the head mask.

1. Nonlinear Anisotropic Diffusion: These are iterative, "tunable" filters introduced by Perona and Malik [37]. Gerig et al. used such filters to enhance MR images [20]. Sapiro and Tannenbaum used a similar technique to perform edge preserving smoothing of MR images [39]. Others have shown that diffusion filters can be used to enhance and detect object edges within images.
2. Automatic Threshold: Once each MRI slice has been diffused we segment the brain using a single automatically found threshold. We observed that the regularization of brain voxels achieved by diffusion filtering results in a brain voxel distribution that is close to normal for T2-weighted and even PD images. Thus the threshold level is determined by fitting a Gaussian curve to the histogram of the diffused volume. For PD and T2-weighted slices, the threshold is chosen at 2 standard deviations below the mean [8]. For T1- weighted axially displayed images, the threshold is chosen at the intensity at the minimum value in the brain histogram plot, which corresponds to about 0.5 standard deviations below the mean of the fitted Gaussian. Fig. 5 shows the voxel-intensity histogram of a diffused T2-weighted volume with the best-fit Gaussian curve and threshold level overlaid. Fig. 6 shows a slice of the binary mask produced by the threshold.

3. Mask Refinement: The binary mask produced by automatic thresholding contains misclassified regions, such as the eyes these regions are removed from each slice using morphology and spatial information provided by the head mask. First, holes are filled within each region of the mask. Next, binary erosion is performed to separate weakly connected regions.

C. Generate Final Brain Mask

Given the initial brain mask as a seed, we use an active contour model algorithm, extended from the "Snakes" algo- rithm introduced by Kass et al. [25], to locate the boundary between the brain and the intracranial cavity. The algorithm deforms the contours defined by the perimeter of the initial brain mask to lock onto the edge of the brain. Each active contour is defined as an ordered collection of points in the image plane.

IV. RESULTS

The proposed method yields the following results as shown in Figure 1 to Figure 6.

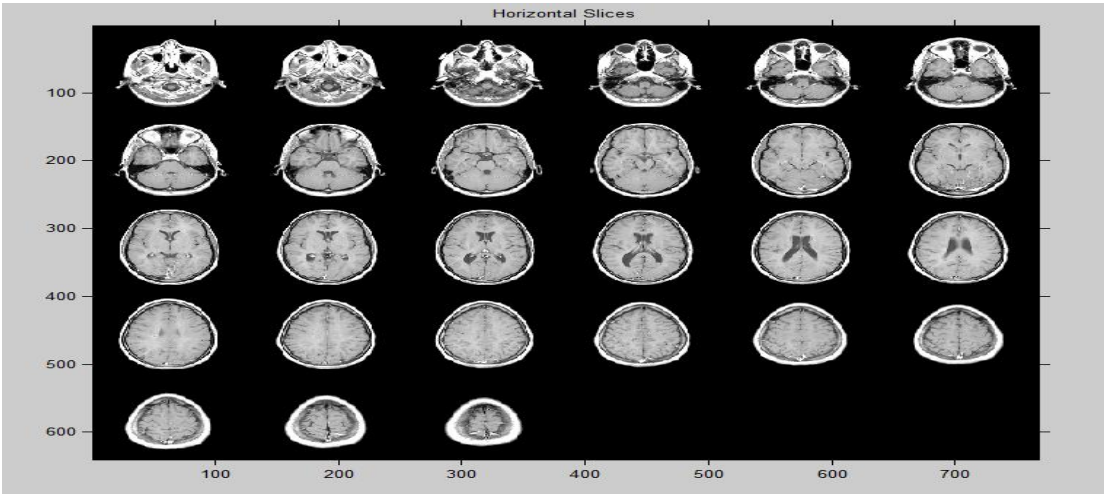

Figure 1. Horizontal Slices of MRI

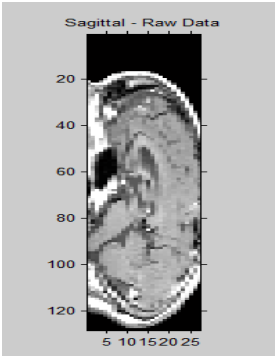

Figure 2. Sagittal Slice from Horizontal Slices of MRI

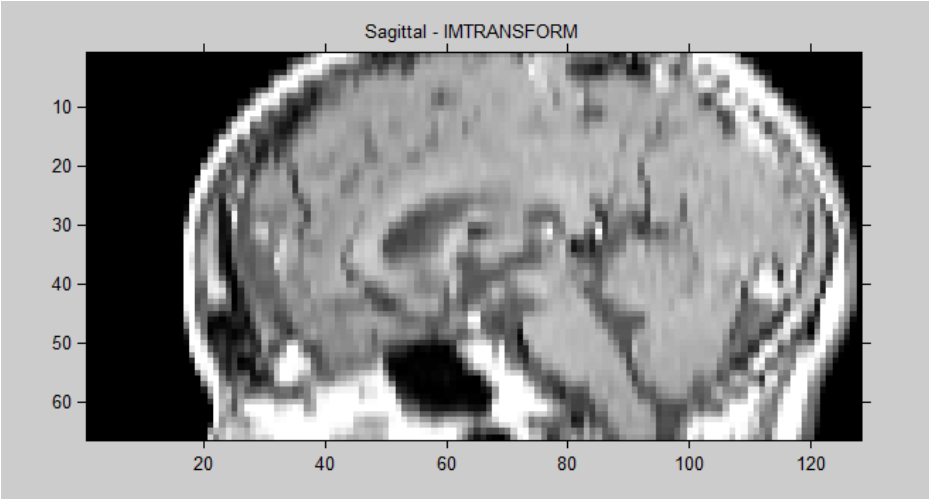

Figure 3. Sagittal Slice transform

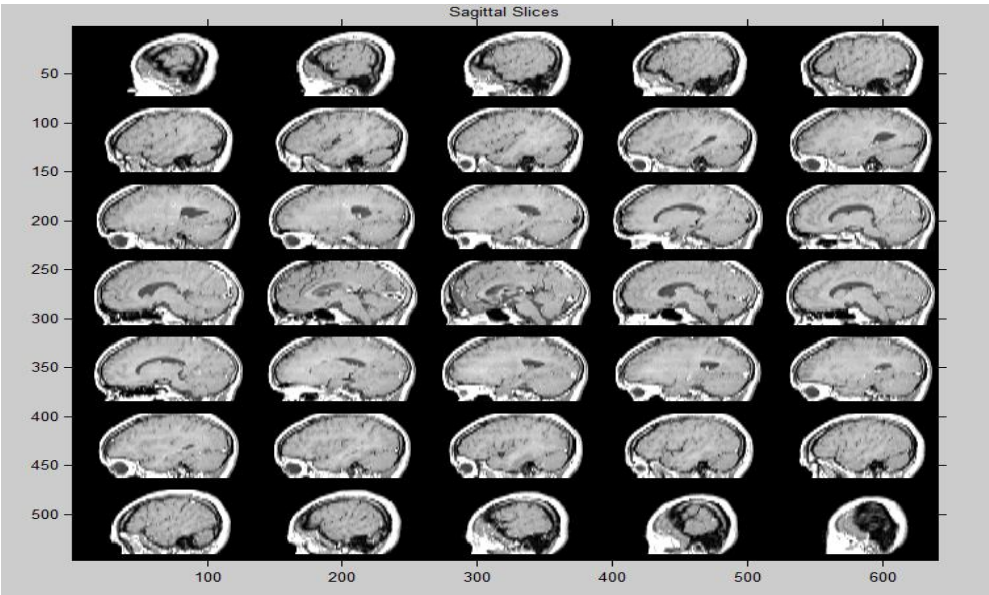

Figure 4. Sagittal Slices from MRI

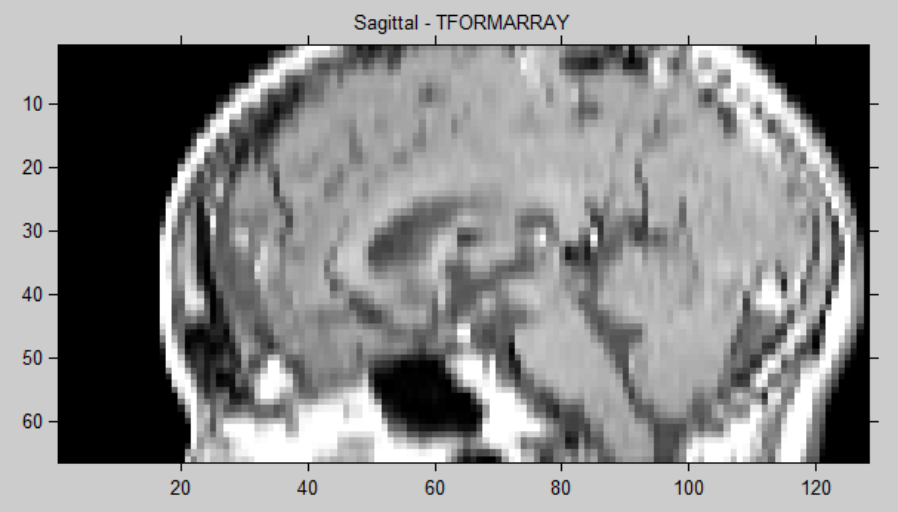

Figure 5. Segmented brain image from MRI

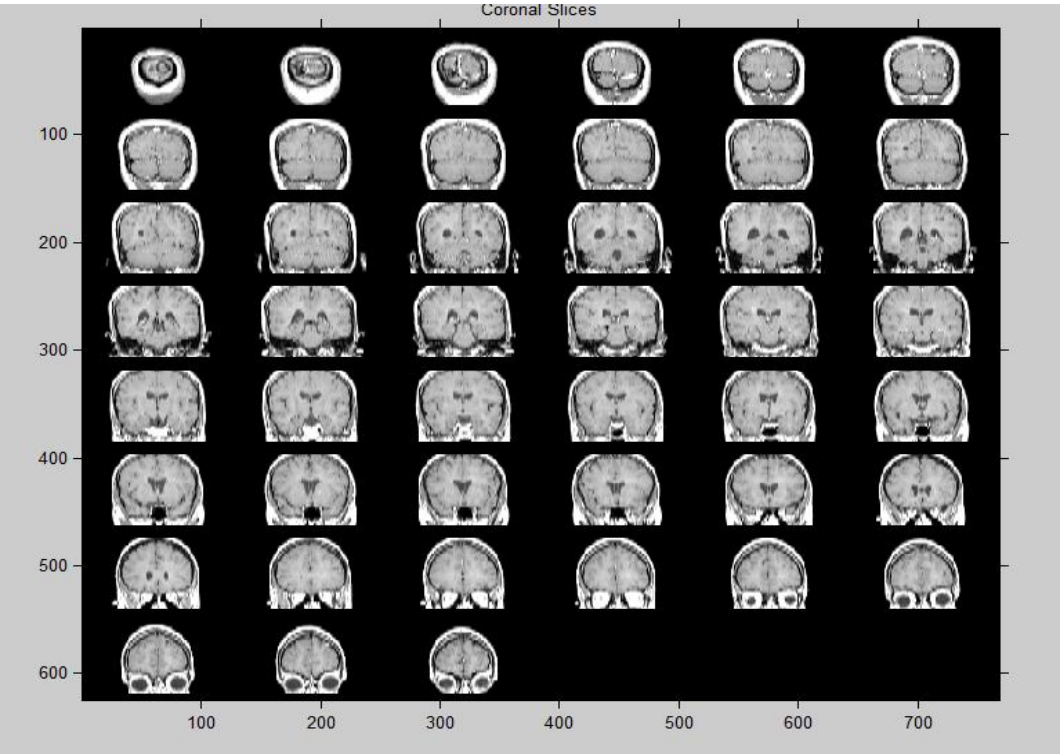

Figure 6. Coronal Slices from MRI

V. CONCLUSION

We have introduced a novel, fully automatic intracranial boundary detection algorithm that has proven effective on clinical and research MRI data sets acquired from several different scanners. The algorithm consists of three incremental steps the first step uses histogram analysis to localize the brain. The second step uses nonlinear anisotropic diffusion and automatic thresholding to create a mask that isolates the brain within the detected head region. Using this mask as a seed, the final step employs an active contour model algorithm to detect the intracranial boundary. This algorithm has proven robust in the presence of RF in homogeneity and partial volume effects.

Our MRI brain segmentation algorithm is in regular use for studies of Multiple Sclerosis lesions, for studies of MRI- PET registration, and for studies involving image compression, where the nonbrain region is automatically given a higher compression ratio than the brain region in the images.

We plan to work with the research 3-D sagittal MP-RAGE volumes, to determine good diffusion filter parameters so that a single threshold can be found for the brain, as our algorithm currently fails to include all the cortical regions of the brain for these images.

We also plan to extend the principles generated for auto- matic brain segmentation to the problem of lung segmentation for use in studies of lung diseases such as cystic fibrosis and emphysema, where the volume of the lungs is needed. A reliable consistent method for outlining the lungs is required for MR chest images. Early results with MR images are promising, and will be continued.

References

1. G. B. Aboutanos and B. M. Dawant, "Automatic brain segmentation and validation: Image-based versus atlas-based deformable models," in Proc. SPIE-Medical Imaging 1997, Feb. 1997, vol. 3034, pp. 299–310.
2. L. Alvarez, P.-L. Lions, and J.-M. Morel, "Image selective smoothing and edge detection by nonlinear diffusion," SIAM J. Number Anal., vol. 29, no. 3, pp. 845–866, June 1992.
3. T. Arden and J. Poon, WiT User's Guide. Logical Vision Ltd., Burnaby, Canada, Oct. 1993, Version 4.1.
4. M. S. Atkins and B. Mackiewich, "Automatic segmentation of the brain in MRI," in Proc. Visualization in Biomedical Computing'96,Sept. 1996, vol. 1131, pp. 210–216.
5. M. S. Atkins, T. Zuk, B. Johnston, and T. Arden, "Role of visual languages in developing image analysis algorithms," in Proc. IEEE Conf. Visual Languages, St. Louis, MO, Oct. 1994, pp. 262–269.
6. C. I. Attwood, G. D. Sullivan, and K. D. Baker, "Recognizing cortical sulci and gyri in MR images," in Proc. British Machine Vision Conf., P. Mowforth, Ed., 1991.
7. J. C. Bezdek, L. O. Hall, and L. P. Clarke, "Review of MR image segmentation techniques using pattern recognition," Med. Phys., vol. 20, no. 4, pp. 1033–1048, 1993.
8. M. E. Brummer, R. M. Mersereau, R. L. Eisner, and R. R. J. Lewine, "Automatic detection of brain contours in MRI data sets," IEEE Trans. Med. Imag., vol. 12, pp. 153–166, June 1993.
9. A. Chakraborty, L. H. Staib, and J. S. Duncan, "An integrated approach to boundary finding in medical images," in Proc. IEEE Workshop on Biomedical Image Analysis, Los Alamos, CA, June 1994, pp. 13–22.
10. V. Chalana, W. Costa, and Y. Kim, "Integrating region growing and edge detection using regularization," in Proc. SPIE Conf. Medical Imaging, 1995.
11. L. P. Clarke, R. P. Velthuizen, M. A. Camacho, J. J. Heine, M. Vaidyanathan, L. O. Hall, R. W. Thatcher, and M. L. Silbiger, "MRI segmentation: Methods and applications," Magn. Reson. Imag., vol. 13, no. 3, pp. 343–368, 1995.
12. H. E. Cline, W. E. Lorensen, R. Kikinis, and F. Jolesz, "Threedimensional segmentation of MR images of the head using probability and connectivity," J. Comput. Assist. Tomogr., vol. 14, no. 6, pp. 1037–1045, Nov./Dec. 1990.
13. D. L. Collins, G. Le Goualher, R. Venugopal, A. Caramanos, A. C. Evans, and C. Barillot, "Cortical constraints for nonlinear cortical registration," in Proc. Visualization in Biomedical Computing'96, Sept. 1996, vol. 1131, pp. 307–316.
14. C. A. Davatzikos and J. L. Prince, "An active contour model for mapping the cortex," IEEE Trans. Med. Imag., vol. 14, pp. 65–80, Mar. 1995.
15. D. Dean, P. Buckley, F. Bookstein, J. Kamath, D. Kwon, L. Friedman, and C. Lys, "Three dimensional MR-based morphometric comparison of schizophrenic and normal cerebral ventricles," in Proc. Visualization in Biomedical Computing'96, Sept. 1996, vol. 1131, pp. 363–372.
16. P. Van den Elsen, J. B. A. Maintz, E.-J. D. Pol, and M. Viergever, "Automatic registration of CT and MR brain images using correlation of geometrical features," IEEE Trans. Med. Imag., vol. 14, pp. 384–395, June 1995.
17. W. A. Edelstein, P. A. Bottomley, and L. M. Pfeifer, "A signal-to-noise calibration procedure for NMR imaging systems," Med. Phys., vol. 11, no. 2, pp. 180–185, 1984.
18. P. A. Freeborough and N. C. Fox, "Assessing patterns and rates of brain atrophy by serial MRI: A segmentation, registration, display and quantification procedure," in Proc. Visualization in Biomedical Computing'96, Sept. 1996, vol. 1131, pp. 419–428.
19. Y. Ge, J. M. Fitzpatrick, B. Dawant, J. Bao, R. Kessler, and R. Margolin, "Accurate localization of cortical convolutions in MR brain images," IEEE Trans. Med. Imag., vol. 15, pp. 418–428, Aug. 1996.
20. G. Gerig, O. K¨ubler, R. Kikinis, and F. A. Jolesz, "Nonlinear anisotropic filtering of MRI data," IEEE Trans. Med. Imag., vol. 11, no. 2, pp. 221–232, June 1992.
21. M. Henkelman, "Measurement of signal intensities in the presence of noise in MR images," Med. Phys., vol. 12, no. 2, pp. 232–233, 1985.
22. B. Johnston, M. S. Atkins, and K. S. Booth, "Partial volume segmentation in 3-D of lesions and tissues in magnetic resonance images," in Proc. SPIE-Medical Imaging 1994, Bellingham, WA, 1994, vol. 2167, pp. 28–39,
23. B. Johnston, M. S. Atkins, B. Mackiewich, and M. Anderson, "Segmentation of multiple sclerosis lesions in intensity corrected multispectral MRI," IEEE Trans. Med. Imag., vol. 15. pp. 154–169, Apr. 1996.

24. T. Kapur, W. E. L. Grimson, W. M. Wells III, and R. Kikinis, "Segmentation of brain tissue from magnetic resonance images," Med. Imag. Anal., vol. 1, no. 2, 1996.
25. M. Kass, A. Witkin, and D. Terzopoulos, "Snakes: Active contour models," Inte. J. Comput. Vision, pp. 321–331, 1988.
26. F. Lachmann and C. Barillot, "Brain tissue classification from MRI data by means of texture analysis," in Proc. SPIE: Medical Imaging VI: Image Processing, Chapel Hill, N.C., 1992, vol. 1652, pp. 72–83.
27. C. Li, D. B. Godlgof, and L. O. Hall, "Knowledge-based classification and tissue labeling of MR images of human brain," IEEE Trans. Med. Imag., vol. 12, pp. 740–750, Dec. 1993.
28. H. Li, R. Deklerk, B. De Cuyper, A. Hermanus, E. Nyssen, and J. Cornelis, "Object recognition in brain CT-scans: Knowledge-based fusion of data from multiple feature extractors," IEEE Trans. Med. Imag., vol. 14, pp. 212–229, June 1995.
29. K. O. Lim and A. Pfefferbaum, "Segmentation of MR brain images into cerebrospinal fluid spaces, white and gray matter," J. Comput. Assist. Tomogr., vol. 13, no. 4, pp. 588–593, July/Aug. 1989.
30. S. Lobregt and M. Viergever, "A discrete dynamic contour model," IEEE Trans. Med. Imag., vol. 14, pp. 12–24, Mar. 1995.
31. A. Lundervold and G. Storvik, "Segmentation of brain parenchyma and cerebrospinal fluid in multipspectral magnetic resonance images," IEEE Trans. Med. Imag., vol. 14, pp. 339–349, June 1995.
32. B. Mackiewich, "Intracranial boundary detection and radio frequency correction in magnetic resonance images," M.S. thesis, Simon Fraser Univ., Burnaby, B.C., Canada, Aug. 1995.
33. N. Nordstr¨om, "Biased anisotropic diffusion—A unified generalization and diffision aapproach to edge detection," Image Vision Comput., vol. 8, no. 4, pp. 318–327, 1990.
34. F. Pannizzo, M. J. B. Stallmeyer, J. Friedman, R. J. Jennis, J. Zabriskie, C. Pland, R. Zimmerman, J. P. Whalen, and P. T. Cahill, "Quantitative MRI studies for assessment of multiple sclerosis," Magn. Reson. Med., vol. 24, pp. 90–99, 1992.
35. D. W. Paty, "Interferon beta-1b in the treatment of multiple sclerosis: Final outcome of the randomized controlled trial," Neurol., vol. 45, pp. 1277–1285, July 1995.
36. D. W. Paty and D. K. B. Li, "Interferon beta-1b is effective in relapsingremitting multiple sclerosis. ii. MRI analysis results of a multicenter, randomized, double-blind, placebo-controlled trial," Neurol., vol. 43, pp. 662–667, Apr. 1993.
37. P. Perona and J. Malik, "Scale-space and edge detection using anisotropic diffusion," IEEE Trans. Pattern Anal. Machine Intell., vol. 12, pp. 629–639, July 1990.
38. S. Ranganath, "Contour extraction from cardiac MRI studies using snakes," IEEE Trans. Med. Imag., vol. 14, pp. 328–338, June 1995.
39. G. Sapiro and A. Tannenbaum, "Edge preserving geometric smoothing of MRI data," Univ. Minnisota, Dept. of Electrical Engineering, Tech. Rep., Apr. 1994.
40. J. W. Snell, M. B. Merickel, J. M. Ortega, J. C. Goble, J. R. Brookeman, and N. F. Kassell, "Segmentation of the brain from 3-D MRI using a hierarchical active surface template," in Proc. SPIE Conf. Medical Imaging, 1994.
41. L. H. Staib and J. S. Duncan, "Boundary finding with parametrically deformale models," IEEE Trans, Pattern Anal. Machine Intell., Nov. 1992.
42. R. R. Stringham, W. A. Barrett, and D. C. Taylor, "Probabilistic segmentation using edge detection and region growing," in Proc. SPIE: Visualization in Biomedical Computing 1992, Chapel Hill, N.C., 1992, vol. 1808, pp. 40–51.
43. H. Suzuki and J. Toriwaki, "Automatic segmentation of head MRI images by knowledge guided thresholding," Computerized Med. Imag., Graphics, vol. 15, no. 4, pp. 233–240, July–Aug. 1991.
44. D. R. Thedens, D. J. Skorton, and S. R. Fleagle, "Methods of graph searching for border detection in image sequences with applications to cardiac MRI," IEEE Trans. Med. Imag., vol. 14, pp. 42–55, Mar. 1995.
45. K. L. Vincken, A. S. E. Koster, and M. A. Viergever, "Probabilistic multiscale image segmentation—set-up and first results," in Proc. SPIE: Medical Imaging VI: Image Processing, Chapel Hill, N.C., 1992, vol. 1808, pp. 63–77.
46. W. M. Wells, III, W. E. L. Grimson, R. Kikinis, and F. A. Jolesz, "Adaptive segmentation of MRI data," IEEE Trans. Med. Imag., vol. 15, pp. 429–443, Aug. 1996.
47. A. P. Zijdenbos, B. M. Dawant, R. A. Margolin, and A. C. Palmer, "Morphometric analysis of white matter lesions in MR images: Method and validation," IEEE Trans. Med. Imag., vol. 13, p. 4, pp. 716–724, Dec. 1994.

